

Analyzing Wildland Fire Smoke Emissions Data Using Compositional Data Techniques

David Weise¹, Javier Palarea-Albaladejo², Timothy J. Johnson³, and Heejung Jung⁴

¹USDA Forest Service

²Biomathematics and Statistics Scotland

³Pacific Northwest National Laboratory

⁴University of California, Riverside

November 22, 2022

Abstract

By conservation of mass, the mass of wildland fuel that is pyrolyzed and combusted must equal the mass of smoke emissions, residual char and ash. For a given set of conditions, these amounts are fixed. This places a constraint on smoke emissions data which violates key assumptions for many of the statistical methods ordinarily used to analyze these data such as linear regression, analysis of variance, and t-tests. These data are inherently multivariate, relative, and non-negative parts of a whole and are then characterized as so-called compositional data. This paper introduces the field of compositional data analysis to the biomass burning emissions community and provides examples of statistical treatment of emissions data. Measures and tests of proportionality, unlike ordinary correlation, allow one to coherently investigate associations between parts of the smoke composition. An alternative method based on compositional linear trends was applied to estimate trace gas composition over a range of combustion efficiency which reduced prediction error by 4 percent while avoiding use of modified combustion efficiency as if it were an independent variable. Use of log-ratio balances to create meaningful contrasts between compositional parts definitively stressed differences in smoke emissions from fuel types originating in the southeastern and southwestern U.S. Application of compositional statistical methods as an appropriate approach to account for the relative nature of data about the composition of smoke emissions and the atmosphere is recommended.

Hosted file

agusupporting-information weise et al.docx available at <https://authorea.com/users/537272/articles/599279-analyzing-wildland-fire-smoke-emissions-data-using-compositional-data-techniques>

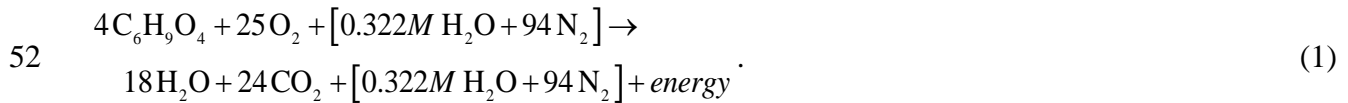
17 **Abstract**

18 By conservation of mass, the mass of wildland fuel that is pyrolyzed and combusted must
19 equal the mass of smoke emissions, residual char and ash. For a given set of conditions, these
20 amounts are fixed. This places a constraint on smoke emissions data which violates key
21 assumptions for many of the statistical methods ordinarily used to analyze these data such as
22 linear regression, analysis of variance, and t-tests. These data are inherently multivariate,
23 relative, and non-negative parts of a whole and are then characterized as so-called compositional
24 data. This paper introduces the field of compositional data analysis to the biomass burning
25 emissions community and provides examples of statistical treatment of emissions data. Measures
26 and tests of proportionality, unlike ordinary correlation, allow one to coherently investigate
27 associations between parts of the smoke composition. An alternative method based on
28 compositional linear trends was applied to estimate trace gas composition over a range of
29 combustion efficiency which reduced prediction error by 4 percent while avoiding use of
30 modified combustion efficiency as if it were an independent variable. Use of log-ratio balances
31 to create meaningful contrasts between compositional parts definitively stressed differences in
32 smoke emissions from fuel types originating in the southeastern and southwestern U.S.
33 Application of compositional statistical methods as an appropriate approach to account for the
34 relative nature of data about the composition of smoke emissions and the atmosphere is
35 recommended.

36 **1 Introduction**

37 Wildland fire is a complex phenomenon of chemical and physical processes. Two of the
38 chemical processes which are key to wildland fire are pyrolysis and combustion (Shafizadeh,

39 1984; Ward, 2001). During pyrolysis, a solid wildland fuel is heated and breaks down into
 40 constituent parts consisting of gases, tars and a solid material called char (Di Blasi, 2008).
 41 During combustion, pyrolysis products react with oxygen releasing energy and a large
 42 assortment of gaseous and solid chemical compounds (e.g. Akagi et al., 2011; Andreae & Merlet,
 43 2001; May et al., 2014). Oxidation reactions involving atmospheric gases such as nitrogen occur
 44 (Crutzen & Brauch, 2016; Lobert et al., 1990). By conservation of mass, the mass of the products
 45 is equal to the sum of the masses of the reactants. For the moment we assume that all products
 46 can be measured with complete accuracy. The measured masses of the individual products
 47 cannot exceed the total mass and are thus numerically related. Measuring a subset of the
 48 complete list of products simply makes the total mass unknown but does not change the inherent
 49 numerical dependency. For example, a simplified balanced global reaction describing
 50 combustion of wood containing water and no inorganic content, shows 1 kg dry wood ($M=0$)
 51 produces 1.82 kg CO₂ and 0.32 kg H₂O for a total mass of products of 2.14 kg (Byram, 1959)



53 Because of the chemical complexity of wood, Byram approximated the proportion of C,
 54 H, and O atoms in wood by C₆H₉O₄. Complete combustion with no dissociation is an idealized
 55 situation which explains the maximum product mass possible. Incomplete combustion and
 56 thermal dissociation will yield additional products and less CO₂. The foliage of woody plants has
 57 a different chemical composition from the wood component which can affect both combustion
 58 and combustion products (Hough, 1969; Jolly et al., 2016; Rogers et al., 1986). The addition of
 59 elements such as N and S, and a host of other elements (many inorganic) to the wood, along with
 60 inclusion of a) the oxidation of atmospheric N by fire (Paul et al., 2008) as well as b) incomplete

61 combustion changes Eq.(1) but does not change conservation of mass. The total mass of the
 62 products (T) can be partitioned to consist of CO, CO₂, particulate matter (PM), other gases, char
 63 and ash

$$64 \quad T = \text{CO} + \text{CO}_2 + \text{other gases} + \text{PM} + \text{char} + \text{ash} . \quad (2)$$

65 If the masses in Eq. (2) are transformed into mass ratios by dividing by the total of CO and CO₂
 66 as in

$$67 \quad \begin{aligned} \frac{T}{\text{CO} + \text{CO}_2} &= \frac{\text{CO}_2 + \text{CO} + \text{other gases} + \text{PM} + \text{char} + \text{ash}}{\text{CO} + \text{CO}_2} \\ &= \frac{\text{CO}_2}{\text{CO} + \text{CO}_2} + \frac{\text{CO}}{\text{CO} + \text{CO}_2} + \frac{\text{other gases}}{\text{CO} + \text{CO}_2} + \frac{\text{PM}}{\text{CO} + \text{CO}_2} + \frac{\text{char}}{\text{CO} + \text{CO}_2} + \frac{\text{ash}}{\text{CO} + \text{CO}_2} , \quad (3) \\ &= MCE + \frac{\text{CO}}{\text{CO} + \text{CO}_2} + \frac{\text{other gases}}{\text{CO} + \text{CO}_2} + \frac{\text{PM}}{\text{CO} + \text{CO}_2} + \frac{\text{char}}{\text{CO} + \text{CO}_2} + \frac{\text{ash}}{\text{CO} + \text{CO}_2} \end{aligned}$$

68 it can be easily seen that modified combustion efficiency $MCE = \text{CO}_2 / (\text{CO} + \text{CO}_2)$ is part of the
 69 total and numerically dependent on the other parts because T is fixed. The above example places
 70 the masses on a relative basis to the amount of CO and CO₂ produced by a fire, demonstrably
 71 two of the three primary products (water being the third). Emissions data have been expressed as
 72 relative measures such as emission ratios and emission factors, concentrations, mixing ratios,
 73 mole fractions, mass fractions, and volume fractions for a very long time (e.g. Darley et al.,
 74 1966; Gerstle & Kemnitz, 1967). However, the statistical properties of relative data have not
 75 typically been considered when these data have been analyzed. Compositional data analysis
 76 (CoDA) is an approach that explicitly considers the statistical properties of relative data
 77 (Aitchison, 1986). Compositional data are contained in the positive orthant of multidimensional
 78 real space (Barceló-Vidal et al., 2001). [An orthant is the multidimensional analogue of a
 79 quadrant in the more familiar two-dimensional Cartesian space.] A recent paper presented
 80 analysis of emissions data using positive matrix factorization which recognized the non-negative

81 nature of emissions data (Sekimoto et al 2018). From a compositional point of view,
82 stoichiometric equations such as (1) have characteristics that discourage, for example, measuring
83 association (correlation) between parts of the composition in the ordinary way (Egozcue et al.,
84 2014).

85 Individual gases produced during pyrolysis and combustion have long been associated
86 with the different phases or conditions (pre-ignition, flaming, smoldering, mixed phase) under
87 which the pyrolysis and combustion have occurred (Lobert & Warnatz, 1993; Tangren et al.,
88 1976). Combustion efficiency (CE) and MCE are indices developed to describe the completeness
89 of the conversion of the carbon contained in the fuel to CO₂ (Ward et al., 1980; Ward & Hao,
90 1991; Yokelson et al., 1997). Theoretically CE includes all carbon produced; however, the
91 challenge to account for all products and the predominance of CO₂ and CO in smoke emissions
92 led to the development of MCE (Ward & Hao, 1991). It has become common practice to
93 correlate emission factors of products other than CO₂ and CO with MCE (e.g. Amaral et al.,
94 2014; Burling et al., 2010; Ferek et al., 1998; Goode et al., 2000; Janhäll et al., 2010;
95 McMeeking et al., 2009; Shen et al., 2013; Urbanski, 2013; Ward & Hao, 1991; Yokelson et al.,
96 2013) using ordinary linear regression. While linking combustion products to CE and MCE is
97 physically sound, the approach to statistical analysis has to date often ignored the intrinsic
98 multivariate and relative nature of these data. As shown above by Eq. (3), MCE as an
99 explanatory variable is automatically correlated to every other wildland fire emission (response
100 variable) by its formulation, not because of physical causation.

101 Aitchison (2003) showed for illustration how two scientists examining the correlation
102 between animal, vegetable, mineral, and water proportions of a sample can arrive at very
103 different correlations (and conclusions) if one scientist dried the sample removing all water

104 before calculating the correlations between the components. We present a similar example
105 (Table 1) using emission factors previously reported (Radke et al., 1988). The original emission
106 factors (g/kg) comprise a composition of D parts which were put on a consistent relative scale by
107 applying the closure operation

$$108 \quad C(\mathbf{x}) = \frac{[x_1, x_2, \dots, x_D]}{\sum_{i=1}^D x_i} \quad (4)$$

109 which divides the emission for each gas (x_i) by the sum of emissions and express the data as
110 fractions of a fixed total, this being 1 by default to be expressed in proportions but in general any
111 other total by simple multiplication (e.g. $C(\mathbf{x}) \cdot 10^2$ for percentages or $C(\mathbf{x}) \cdot 10^6$ for parts per
112 million). After closure, the CO₂ emission factor of 1664 g/kg becomes the proportion 0.948.

113

114 **Table 1. Example illustrating how ordinary correlation of relative data such as emission**
 115 **factors produces spurious results. Data from Radke et al. (1988).**

Emission factors (g/kg)								
	CO	CO ₂	CH ₄	C ₃ H ₆	C ₂ H ₆	C ₃ H ₈	C ₂ H ₃	PM
	74	1664	2.4	0.58	0.35	0.21	0.32	13.5
	75	1650	3.6	0.46	0.55	0.32	0.21	23.0
	106	1626	3.0	0.70	0.60	0.25	0.22	6.1
	89	1637	2.6	0.08	0.56	0.42	0.19	20.2
Full composition (after closure C)								
	4.22E-02	9.48E-01	1.37E-03	3.30E-04	1.99E-04	1.20E-04	1.82E-04	7.69E-03
	4.28E-02	9.41E-01	2.05E-03	2.62E-04	3.14E-04	1.83E-04	1.20E-04	1.31E-02
	6.08E-02	9.33E-01	1.72E-03	4.02E-04	3.44E-04	1.43E-04	1.26E-04	3.50E-03
	5.09E-02	9.35E-01	1.49E-03	4.57E-05	3.20E-04	2.40E-04	1.09E-04	1.15E-02
No CO ₂ subcomposition								
	8.10E-01		2.63E-02	6.35E-03	3.83E-03	2.30E-03	3.50E-03	1.48E-01
	7.27E-01		3.49E-02	4.46E-03	5.33E-03	3.10E-03	2.04E-03	2.23E-01
	9.07E-01		2.57E-02	5.99E-03	5.13E-03	2.14E-03	1.88E-03	5.22E-02
	7.87E-01		2.30E-02	7.08E-04	4.95E-03	3.72E-03	1.68E-03	1.79E-01
Pearson correlation								
CO ₂	Full (F)		-0.25	0.18	-0.93	-0.49	0.82	0.25
CO	F	-0.88	-0.01	0.19	0.69	0.06	-0.44	-0.68
	Sub (S)		-0.59	0.40	-0.10	-0.67	-0.03	-1.00
CH ₄	F			0.19	0.58	0.12	-0.53	0.31
	S			0.29	0.37	0.00	0.01	0.53
C ₃ H ₆	F				-0.17	-0.92	0.51	-0.71
	S				-0.36	-0.95	0.61	-0.47
C ₂ H ₆	F					0.54	-0.93	-0.01
	S					0.38	-0.92	0.09
C ₃ H ₈	F						-0.81	0.65
	S						-0.53	0.72
C ₂ H ₃	F							-0.34
	S							0.01

116

117 Regardless of the total, it is important to note that the resulting relativized data vector is
 118 equivalent to the original emission factors and lives in what is known as a D -part simplex and,
 119 hence, statistical analysis on any equivalent representation of the data should provide the same
 120 results. In the example in Table 1, $D = 8$ for the full composition. The familiar Pearson
 121 correlation coefficient (r) was then calculated for all pairs of gases. In the full composition, CO
 122 was negatively correlated with CO₂ ($r=-0.88$), positively correlated with C₂H₆ (0.69) and not
 123 correlated with C₃H₈ (0.06). The emission factor for CO₂ was then removed from the full

124 composition as if it had not been measured and the closure operation was performed on the
125 subcomposition (subset), producing the second set of values, and correlation between the pairs
126 was calculated. Correlation coefficients which changed appreciably are highlighted. Note that
127 CO is now negatively correlated with C_3H_8 (-0.67) and not correlated with C_2H_6 (-0.10).
128 Similarly, CH_4 was negatively correlated with C_2H_3 in the full composition (-0.53) and not
129 correlated (0.01) when CO_2 is not in the composition. The point of this illustration is that this
130 index (Pearson correlation coefficient) that is generally trusted as a measure of pairwise
131 association can produce different results depending on something that should not affect it. This is
132 an artifact not related to the actual relationship between the variables. Hence, it is not a reliable
133 measure with this type of data, regardless of the magnitude of the difference in a particular case,
134 which will be arbitrarily big or small. That the interpretation of these changing correlations could
135 lead to spurious conclusions is well known (Pearson, 1896). This simple example illustrates the
136 problem using correlation with relative data. Linear regression utilizes correlation so it is also
137 affected by this constraint: measuring associations in terms of proportionality is a coherent and
138 meaningful alternative to ordinary correlation for compositional data (Egozcue et al., 2014,
139 2018; Lovell et al., 2015).

140 The use of predictions resulting from correlations and linear regressions that do not
141 account for the relative nature of emissions data may produce misleading estimates in emissions
142 inventories developed by various regulatory agencies. This is true for operational tools such as
143 the Fire Emissions Production Simulator and its successors (Anderson et al., 2004) as well as the
144 First Order Fire Effects Model and its successors. It also represents just one of many sources of
145 potential error in emissions calculations (Ottmar et al., 2008; Surawski et al., 2016). In this paper
146 we therefore propose a different approach to analyze emissions data that reflects their

147 compositional nature. A well-principled methodological body to analyze compositional data has
148 been developed in the past 30 years and this is an active area of statistical research so we have
149 chosen to apply it to fire emissions data, in particular gas-phase emissions. Interestingly, it has
150 been successfully applied in varied fields, but appears to have seldom been applied to
151 combustion or emissions data (Bandein-Roche, 1994; Billheimer, 2001; Buccianti &
152 Pawlowsky-Glahn, 2006; Speranza et al., 2018). A recent analysis that recognized

153 The relative nature of emissions data defines emissions data as compositional data which
154 are coherently analyzed using CoDA (Aitchison, 1986; Barceló-Vidal et al., 2001; Lovell et al.,
155 2015; Pawlowsky-Glahn et al., 2015b). CoDA methodology has three underlying principles. The
156 first is scale invariance—vectors with proportional positive components represent the same
157 composition, and form what is known as an equivalence class. This means changing the units
158 should not change relative relationships between the parts nor affect results and scientific
159 conclusions. The second is that inferences about subcompositions, i.e. smaller compositions
160 formed from subsets of parts, must not contradict the inferences from the full composition (as in
161 the example in Table 1). The third principle states that the order of the parts of the composition
162 must not affect the inferences. While the initial work on CoDA explicitly assumed in the
163 definition of a composition that the parts sum (are closed) to a constant total, theory has
164 developed to show that this is only a particular representation of the data in a simplex and
165 equivalent non-closed compositions carry the same relative information (Barcelo-Vidal &
166 Martín-Fernández, 2016). So the “conservation of mass” argument presented earlier is not
167 necessary for emissions data to be considered compositional as shown by Egozcue (2009). The
168 structural relationship and interdependence between MCE and other emissions as shown in (3)
169 still holds.

170 Aitchison (1982) showed that a meaningful approach to compositional data is to analyze
 171 log-ratios of the parts which carry the relative information. Aitchison (1986) defined the two
 172 basic operations of perturbation (\oplus , analogous to addition or translation with ordinary real-
 173 valued data)

$$174 \quad \mathbf{z} = \mathbf{x} \oplus \mathbf{p} = C[x_1 \cdot p_1, \dots, x_d \cdot p_d] \quad (5)$$

175 and power transformation (\otimes , analogous to multiplication by a scalar)

$$176 \quad \mathbf{z} = \lambda \otimes \mathbf{x} = C[x_1^\lambda, \dots, x_d^\lambda] \quad (6)$$

177 where \mathbf{x} is the initial composition, \mathbf{p} is a perturbation vector and λ is a constant. These operations
 178 are foundational to CoDA.

179 In CoDA today, in order to use familiar statistical techniques such as exploratory data
 180 analysis, linear regression, multivariate analysis of variance and other multivariate techniques,
 181 the mainstream approach is to transform the parts from the simplex to real numbers using
 182 isometric log-ratio (ilr) coordinates (van den Boogaart & Tolosana-Delgado, 2013; Egozcue &
 183 Pawlowsky-Glahn, 2005; Mateu-Figueras et al., 2011; Pawlowsky-Glahn et al., 2015b). The
 184 linear algebra theory supporting these transformations also provides the underpinnings for
 185 “standard” or “classical” statistics routinely used in the sciences (Graybill, 2002). Several texts
 186 describe the theory and methods of compositional data analysis (Aitchison, 1986; van den
 187 Boogaart & Tolosana-Delgado, 2013; Filzmoser et al., 2018; Pawlowsky-Glahn et al., 2015b;
 188 Pawlowsky-Glahn & Buccianti, 2011). Software to perform compositional data analysis is
 189 available, including the stand-alone point-and-click *CoDaPack* package (Thió-Henestrosa &
 190 Comas, 2016) (<http://www.compositionaldata.com/codapack.php>) and comprehensive libraries
 191 on the open-source R statistical computing system (R Core Team, 2018): *compositions* (van den

192 Boogaart & Tolosana-Delgado, 2013), *robCompositions* (Templ et al., 2011) and *zCompositions*
193 (Palarea-Albaladejo et al., 2014; Palarea-Albaladejo & Martín-Fernández, 2015).

194 The above considerations borne in mind, the objectives of this manuscript are to re-
195 analyze the Burling et al. (2010) emissions factors data to 1) determine if parts (individual gases)
196 were proportional to each other (in place of correlated in the usual way), 2) determine if a
197 compositional linear trend can be used to model the data as combustion efficiency changes (in
198 place of ordinary linear regression using MCE), and 3) determine if the composition of the gases
199 differed between fuel types using analysis of variance within a CoDA framework. We hope to
200 demonstrate that the CoDA approach can shed as much or more light on the relationships in and
201 between the emissions data by applying techniques consistent with the nature of the data instead
202 of using simple linear regression with MCE thus avoiding artifacts derived from the very own
203 nature of the data.

204 **2 Statistical Methods**

205 Burling et al. (2010) reported emission factors for 18 gases measured using an open-path
206 FTIR spectrometer (Burling et al., 2010) and characteristics of the combustion (fuel moisture
207 content, fuel consumption, MCE) for 65 laboratory fires (observations) in 15 different wildland
208 fuel types. Each of the 65 observations comprised a vector $\mathbf{x}_i = [x_1 \dots x_{18}]_i$ where parts $x_1 \dots x_{18}$
209 were the measured emission factors for CO₂, CO, CH₄, C₂H₂, C₂H₄, C₃H₆, CH₃OH, HCOOH,
210 CH₃COOH, HCHO, C₄H₄O, NH₃, NO, NO₂, HONO, HCN, HCl, and SO₂, respectively. In
211 actuality, these 18 gases were a subcomposition of a much larger composition of gaseous and
212 solid emissions sampled from these experimental fires by a variety of methods and instruments
213 described elsewhere (Burling et al., 2010; Chang-Graham et al., 2011; Gilman et al., 2015;

214 Hosseini et al., 2010, 2013; Roberts et al., 2010; Veres et al., 2010; Warneke et al., 2011; Weise
215 et al., 2015; Yokelson et al., 2013). The full composition for this experiment consisted of over
216 100 parts. The data set resulted from a laboratory study at the United States Forest Service's
217 Missoula Fire Sciences Lab (USFS-FSL). This FSL study characterized smoke emissions related
218 to prescribed burning of 15 different shrub and woodland fuel types from the southeastern and
219 southwestern U.S. and described the composition of gas and particulate matter in detail. In the
220 present paper, 18 gases were re-analyzed which had previously been measured using an open-
221 path FTIR spectrometer (Burling et al., 2010) and then adjusted to field values using MCE
222 (Yokelson et al., 2013) While it is possible to measure H₂O (gas) in smoke emissions using FTIR
223 and while it is a significant product of combustion that can influence flame processes (Ferguson
224 et al., 2013), emission factors for H₂O are not typically reported. The gas-phase data analyzed
225 here are originally available as supplementary information to the Yokelson et al. (2013) paper.
226 Furan (C₄H₄O) and hydrochloric acid (HCl) had one and four (1.5 and 6 %) instances of below-
227 detection limit (BDL) values, respectively. In order to facilitate statistical analysis, the log-ratio
228 EM algorithm included in the *zCompositions* package was used to impute the BDL values with
229 realistically small values while accounting for their compositionality (Palarea-Albaladejo &
230 Martín-Fernández, 2015). In the following, we introduce the basic compositional analyses
231 conducted using these data which are analogous to those commonly conducted on emission data.

232 *2.1 Summary statistics and proportionality associations*

233 The data were closed and compositional summary statistics consisting of the center
234 (geometric mean) and the variation array (Aitchison, 1986) were estimated. The center ($\bar{\mathbf{g}}$) is the
235 closed vector of geometric means for each part estimated as

236 $\hat{\mathbf{g}} = C[\hat{g}_1, \hat{g}_2, \dots, \hat{g}_D]$ (7)

237 where $\hat{g}_j = \left(\prod_{i=1}^n x_{ij}\right)^{1/n}$, $j = 1, 2, \dots, D$. While there are different measures for the variability of
 238 compositional data (van den Boogaart & Tolosana-Delgado, 2013), a common summary is given
 239 by the variance (τ_{ij}) of the log-ratio of parts i and j ; the variation matrix \mathbf{V} is a $D \times D$ symmetric
 240 matrix containing elements estimated by

241 $\hat{\tau}_{ij} = \text{var}\left(\ln \frac{x_i}{x_j}\right)$ (8)

242 where i and j range from 1 to D and var is the usual variance. The total (or metric) variance
 243 (Mvar) can be obtained from them as (Egozcue & Pawlowsky-Glahn, 2011; Pawlowsky-Glahn
 244 & Egozcue, 2001):

245
$$\text{Mvar}(\mathbf{x}) = \sum_i \sum_j \hat{\tau}_{ij} = \sum_{i=1}^D \text{var}[\text{clr}_i(\mathbf{x})]$$
 (9)

246 where the centered log-transformation (clr) and its inverse are

247
$$\text{clr}(\mathbf{x}) = \left[\ln \frac{x_1}{g_m(\mathbf{x})}, \ln \frac{x_2}{g_m(\mathbf{x})}, \dots, \ln \frac{x_D}{g_m(\mathbf{x})} \right], \quad g_m(\mathbf{x}) = \left(\prod_{i=1}^D x_i\right)^{1/D}$$
 (10)

$$\text{clr}^{-1}(\mathbf{x}) = C[\exp(\text{clr}(\mathbf{x}))]$$

248 and the metric standard deviation (Mstd) is $\sqrt{\frac{\text{Mvar}}{D-1}}$. In general, the smaller the values of $\hat{\tau}_{ij}$, the
 249 more proportional are the parts involved.

250 For non-compositional data, relationships between variables are ordinarily explored by
 251 examining correlation (parametric or nonparametric) between the variables. For compositional
 252 data, proportionality is the preferred measure to examine relationships between parts of a

253 composition in accordance with their relative scale (Aitchison, 1986; Lovell et al., 2015). As
254 stated in Lovell et al (2015), “*measures of association produce results regardless of the data*
255 *they are applied to-it is up to the analyst to ensure that the measures are appropriate to the*
256 *data.*” They further state that proportional relative abundances imply that the absolute
257 abundances are proportional. Balance association (or b-association for short) was developed as a
258 consistent statistical concept of proportionality (Egozcue et al., 2018). A measure of b-
259 association, ϕ , has been defined and used to formulate a statistical hypothesis test of equality to
260 ± 1 of the slope coefficient of a major or standardized major axis regression model (Warton et al.,
261 2006) relating one log-contrast of parts to another log-contrast. This is the so-called unitary slope
262 test, with significance based on a standard F distribution (Egozcue et al., 2018; Lovell et al.,
263 2015). Rejection of the hypothesis suggests that the data are not compatible with b-association
264 (or proportionality) between the parts; however, it does not distinguish whether the slope is
265 positive or negative. Following Egozcue et al. (2018), we rejected the hypothesis when the
266 estimated slope was negative and reported the p-value as a minus sign (-).

267 2.2 Compositional linear trend analysis

268 Since its introduction *MCE* has frequently been correlated to single emission factors (*EF*)
269 by linear regression $EF = \beta_0 + \beta_1(MCE)$ (Ward & Hao, 1991) which assumed that the predictor
270 variable *MCE* could be treated separately from the response variable *EF*. As shown above in eq.
271 3 this is not the case, so an alternative method to estimate emission factors developed for
272 compositional data was applied instead. Deriving principal components from multivariate data is
273 a common practice. They were used in von Eynatten et al. (2003) to develop the compositional
274 linear trend method which we apply to our data using recently developed R code (Rockwell et

275 al., 2014). The basic idea is that compositional data can be projected onto the first principal
 276 component to produce a linear trend provided that the first principal component explains a large
 277 proportion of the total variance. The projected (or fitted) composition can be transformed back to
 278 the original units (Pawlowsky-Glahn et al., 2015a). We chose to apply this method because it has
 279 been well established that the composition of smoke changes as the combustion efficiency
 280 changes (Byram, 1957). If the linear trend method works, it could potentially be applied to other
 281 data sets to predict composition.

282 When originally developed, the linear trend method was applied to geological data to
 283 model the compositional changes in granitic rocks as they weathered from fresh parent material.
 284 The unweathered parent material served as the starting point of the linear trend which is
 285 formulated in the simplex as

$$286 \quad \mathbf{x} = \mathbf{a} \oplus (k \otimes \mathbf{p}) = \mathbf{C} [a_1 p_1^k, \dots, a_d p_d^k] \quad (11)$$

287 and estimated by

$$288 \quad \hat{\mathbf{x}} = \mathbf{a} \oplus (k \otimes \text{clr}^{-1} [\mathbf{v}_1]) \quad (12)$$

289 where \mathbf{a} is the starting composition, k is the latent trend, \mathbf{p} is a perturbation vector estimated by
 290 $\text{clr}^{-1}(\mathbf{v}_1)$, \mathbf{v}_1 is the first eigenvector derived by noncentral principal component analysis of the
 291 original n observations $\mathbf{x}_1, \dots, \mathbf{x}_n$ after they were adjusted to the starting point \mathbf{a} by
 292 $\text{clr}(\mathbf{x}_1) - \text{clr}(\mathbf{a}), \dots, \text{clr}(\mathbf{x}_n) - \text{clr}(\mathbf{a})$. Noncentral principal component analysis indicates the
 293 variances were maximized relative to \mathbf{a} instead of to the mean (von Eynatten, 2004). The full
 294 mathematical development can be found elsewhere (von Eynatten et al., 2003). The linear trend
 295 method describes changes within a compositional data set that are not attributed to variables

296 external to the composition. In the present study, we evaluated three compositions as the
297 potential starting composition **a**: the highest (High) and lowest (Low) MCE compositions and the
298 center composition of the data set. Linear regressions were not fit for CO and CO₂ since they
299 form MCE. In order to compare the performance of the linear trend to the ordinary linear
300 regression, common error measures were calculated using the observed and predicted emission
301 factors for each gas for each linear regression and linear trend. The estimated values were scaled
302 to the original units (Pawlowsky-Glahn et al., 2015a). The normalized mean absolute error
303 (NMAE) and root mean squared error (RMSE) of the observed and estimated values were
304 calculated using the *modStats* function in R (Carslaw, 2015; Carslaw & Ropkins, 2012). Since
305 multivariate linear regression is the extension of linear regression to data with correlated
306 response variables (Fox & Weisberg, 2018, 2019), we performed a multivariate linear regression
307 with all trace gases except CO and CO₂ as the dependent variables and MCE as the predictor
308 variable. The fitted values from the multivariate linear regression were identical to the individual
309 linear regressions so the error measures were identical and are not presented. Multivariate linear
310 regression, even though it takes into the account the correlation structure between the parts of the
311 composition, was still subject to the fact that the MCE ratio was not independent of the other
312 gases in the mixture. To examine the fits of the linear trend and multivariate linear regression for
313 the entire composition, a coefficient of determination (R_{CLT}^2) for the linear trend (van den
314 Boogaart & Tolosana-Delgado, 2013; Cayuela-Sánchez et al., 2019) and the squared multiple
315 correlation coefficient (R_{LR}^2) for the multivariate linear regression (Mardia et al., 1979) were
316 estimated. The metric standard deviation in the original emission factor units $\exp(\text{Mstd})$ and the
317 root mean squared error of the multivariate linear regression (calculated as the square root of the
318 mean of the trace of the residual matrix) estimated $RMSE_{CLT}$ and $RMSE_{LR}$, respectively.

319 *2.3 Multivariate analysis of variance*

320 Analysis of variance was used to test for differences in the composition of the gases
 321 according to fuel type. Note that because of experimental design deficiencies resulting in a
 322 singular design matrix, it was not possible to consider fuel type and region simultaneously.
 323 Egozcue and Pawlowsky-Glahn (2005) devised a procedure to obtain sets of ilr coordinates by
 324 sequential binary partitioning that can be used for them to represent comparisons between
 325 scientifically meaningful subsets of parts of a composition. These ilr coordinates known as
 326 compositional balances \tilde{z}_k are defined as

$$327 \quad \tilde{z}_k = \sqrt{\frac{r_k s_k}{r_k + s_k}} \ln \frac{\left(x_{i_1} x_{i_2} \dots x_{i_{r_k}}\right)^{1/r_k}}{\left(x_{j_1} x_{j_2} \dots x_{j_{s_k}}\right)^{1/s_k}}, \quad k = 1, \dots, D-1 \quad (13)$$

328 where the log-ratio compares the geometric mean of r_k parts in one subset with the geometric
 329 mean of s_k parts in another subset. Sequential binary partitioning of a composition containing D
 330 parts results in $D-1$ balances $\tilde{z}_k, k = 1, \dots, D-1$. The emissions data were then transformed into
 331 balance coordinates that partitioned the composition into various meaningful subsets of parts.
 332 The matrix used to define the subsets contains 1, -1, or a blank to indicate that the part is in
 333 subset 1 (numerator), subset 2 (denominator) or absent from the log-ratio, respectively. Once the
 334 data were transformed into balance coordinates, analysis of variance was used on them to test for
 335 differences in mean according to fuel type. Given the large number of statistical tests performed
 336 in this analysis, we chose to adjust the p-values to control for false discovery rate (Benjamini &
 337 Hochberg, 1995). Statistical significance was assessed at the usual 5% level.

338 **3 Results and Discussion**

339 *3.1 Summary statistics*

340 MCE ranged from 0.91 for the *lit* fuel type to over 0.98 for the *oas* fuel type. The
341 geometric mean of MCE for the data set was 0.96. [Details of the fuel types and fuel
342 consumption in the individual fires have been presented in the original publications (Burling et
343 al., 2010; Hosseini et al., 2010, 2013)]. Numerical differences in the MCE values reported by
344 Burling et al. (2010) and Yokelson et al. (2013) due to adjustment for field measurements are
345 described in the latter reference. Unsurprisingly, the chemical compositions changed as
346 combustion efficiency decreased from high to low (Table 2). Examination of the compositional
347 makeup of the low MCE, geometric mean MCE, and high MCE revealed that relative abundance
348 of all gases except CO₂, NO, and NO₂ increased as the MCE decreased. By definition, CO₂
349 increases and CO decreases as the MCE increases. Previously reported gas species associated
350 with flaming combustion (higher MCE) included CO₂, NO, NO₂, HCl, SO₂ and HONO; those
351 usually associated with smoldering combustion (lower MCE) include CO, CH₄, NH₃, HCN,
352 C₃H₆, CH₃OH, CH₃COOH, and C₄H₄O (Burling et al., 2010; Goode et al., 2000). Of the species
353 we measured, the remaining ones have been associated with both flaming and smoldering
354 combustion.

355 Large variation in the emission factor for HCl for this data set was previously reported
356 (Burling et al., 2010). The large log-ratio variance associated with HCl was also readily apparent
357 in a biplot (Aitchison & Greenacre, 2002) produced from the first two principal components of
358 the data set (not shown). This can be also seen with its clr-variance (Table 2). The clr-variance
359 for HCl (1.50) was approximately 25 percent of the total variance (6.09). The clr-variances for

360 the remaining 17 parts were similar in size, yet small compared to HCl. While there were several
361 low values of $\hat{\tau}_{ij}$ that suggested proportionality, only a few of the unitary slope tests were not
362 statistically significant (Table 2) suggesting that some of the gases might be pairwise
363 proportional. Potential pairwise proportionality relationships include: 1) propene (C_3H_6) with
364 acetic acid (CH_3COOH), formaldehyde ($HCHO$), furan (C_4H_4O), ammonia (NH_3), and HCN, all
365 of which have been associated with smoldering combustion; and 2) acetic acid with furan,
366 nitrous acid ($HONO$) and hydrocyanic acid (HCN). The mean log-ratios of the five gases
367 potentially proportional with propene ranged from -0.62 (HCN) to 1.61 (acetic acid) suggesting
368 relatively less propene than HCN consistently in the smoke samples and relatively more propene
369 than acetic acid, consistently. While the log-ratio variances for these five gases with propene
370 were similar in size (0.25 to 0.33), the probabilities associated with the F-tests ranged
371 considerably (0.07 to 0.94); the higher probability levels provide better support the potential
372 proportionality of propene with the other hydrocarbons and less support for proportionality with
373 the two N gases (NH_3 , HCN). Note that while the log-ratio variance of CH_3OH with propene was
374 lower than the log-ratio variances for CH_3COOH , $HCHO$, furan, ammonia and HCN , the slope
375 test rejected potential pairwise proportionality. Other smoldering compounds for which results
376 were compatible with proportionality included 3) formaldehyde with methanol, acetic acid, and
377 furan; 4) ethene (C_2H_4) with methane and ammonia; and 5) HCN with methane and furan. Of the
378 gases associated with flaming combustion, CO_2 was potentially proportional with NO_2 , C_2H_2 and
379 $HONO$. It was interesting to note that some gases normally associated with flaming show some
380 level of proportionality with smoldering gases: $HONO$ with acetic acid, SO_2 with CO and
381 ammonia. Because of its large variability, HCl exhibited the lowest proportionality to any other
382 gases in the composition; all tests were rejected since the slope values were negative (J.J.

383 Egozcue et al., 2018). All log-ratio means for HCl were negative which indicated that the
384 proportion of HCl in the compositions was less than the proportions of the other gases.

385 **Table 2. Variation array and center of smoke emissions. The upper right triangular matrix contains estimates of log-ratio variance ($\hat{\tau}_{ij}$) and**
 386 **(probability of F-statistic for slope test of proportionality). The minus (-) sign denotes a negative slope and rejection of the null hypothesis of**
 387 **perfect proportionality. Shading indicates that the hypothesis was not rejected at the 5% significance level suggesting potential**
 388 **proportionality between parts. The lower left triangular matrix contains the log-ratio means. The three bottom rows are the compositional**
 389 **makeup (as proportions) for the lowest, highest, and center MCE values ($\times 10^3$).**

	CO ₂	CO	CH ₄	C ₂ H ₂	C ₂ H ₄	C ₃ H ₆	CH ₃ OH	HCOOH	CH ₃ COOH	HCHO	C ₄ H ₄ O	NH ₃	NO	NO ₂	HONO	HCN	HCl	SO ₂
CO ₂		0.12 (0.00)	0.37 -	0.50 (0.11)	0.43 -	0.69 -	0.65 -	0.92 -	0.73 -	0.71 -	0.63 -	0.24 (0.02)	0.06 (0.00)	0.16 (0.23)	0.23 (0.11)	0.95 -	2.88 (0.00)	0.14 (0.00)
CO	-3.33		0.18 (0.00)	0.33 (0.00)	0.20 -	0.41 -	0.33 -	0.58 -	0.44 -	0.36 -	0.33 -	0.17 (0.02)	0.22 (0.00)	0.21 (0.00)	0.21 (0.00)	0.54 -	2.66 (0.00)	0.10 (0.29)
CH ₄	-7.05	-3.72		0.36 (0.00)	0.08 (0.45)	0.17 (0.00)	0.17 (0.03)	0.51 -	0.31 -	0.27 -	0.35 -	0.15 (0.03)	0.53 -	0.38 -	0.32 -	0.29 (0.00)	2.92 -	0.18 -
C ₂ H ₂	-9.61	-6.28	-2.56		0.28 (0.00)	0.64 -	0.70 -	1.05 -	0.88 -	0.67 -	0.85 -	0.42 (0.00)	0.63 -	0.67 -	0.48 (0.00)	0.87 -	2.78 (0.00)	0.44 (0.00)
C ₂ H ₄	-8.28	-4.95	-1.23	1.33		0.12 (0.00)	0.19 (0.15)	0.49 -	0.33 -	0.24 (0.01)	0.35 -	0.18 (0.15)	0.56 -	0.42 -	0.27 -	0.30 (0.00)	3.13 -	0.21 -
C ₃ H ₆	-9.43	-6.10	-2.37	0.18	-1.14		0.16 (0.04)	0.48 (0.03)	0.29 (0.94)	0.25 (0.49)	0.33 (0.81)	0.30 (0.08)	0.86 -	0.58 -	0.43 -	0.26 (0.07)	3.47 -	0.40 -
CH ₃ OH	-8.48	-5.15	-1.43	1.13	-0.20	0.94		0.21 (0.00)	0.07 (0.00)	0.08 (0.11)	0.17 (0.02)	0.35 -	0.83 -	0.44 -	0.37 -	0.16 (0.00)	3.31 -	0.31 -
HCOOH	-10.11	-6.78	-3.05	-0.50	-1.83	-0.68	-1.63		0.13 (0.00)	0.12 (0.00)	0.22 (0.01)	0.74 -	1.14 -	0.61 -	0.49 (0.00)	0.44 (0.56)	3.81 -	0.59 -
CH ₃ COOH	-7.82	-4.49	-0.76	1.79	0.47	1.61	0.66	2.29		0.09 (0.27)	0.20 (0.85)	0.52 -	0.94 -	0.43 -	0.36 (0.35)	0.28 (0.09)	3.53 -	0.38 -
HCHO	-8.43	-5.10	-1.38	1.18	-0.15	1.00	0.05	1.68	-0.61		0.17 (0.28)	0.51 -	0.93 -	0.48 -	0.36 -	0.28 (0.01)	3.34 -	0.41 -
C ₄ H ₄ O	-10.17	-6.84	-3.12	-0.56	-1.89	-0.75	-1.69	-0.06	-2.35	-1.74		0.45 -	0.81 -	0.52 -	0.46 -	0.33 (0.14)	3.51 -	0.38 -
NH ₃	-8.04	-4.71	-0.99	1.57	0.24	1.38	0.44	2.07	-0.22	0.39	2.13		0.30 (0.00)	0.32 -	0.31 -	0.44 (0.00)	2.93 -	0.15 (0.13)
NO	-6.70	-3.37	0.35	2.91	1.58	2.73	1.78	3.41	1.12	1.73	3.47	1.34		0.28 (0.00)	0.34 (0.00)	1.14 -	3.10 -	0.21 (0.00)

Confidential manuscript submitted to JGR Atmospheres

NO ₂	-7.85	-4.52	-0.79	1.76	0.44	1.58	0.63	2.26	-0.03	0.58	2.32	0.19	-1.15	0.19 (0.59)	0.72	2.87	0.18	
HONO	-8.87	-5.54	-1.82	0.74	-0.59	0.55	-0.39	1.24	-1.05	-0.44	1.30	-0.83	-2.17	-1.02	0.73	3.33	0.21 (0.02)	
HCN	-10.05	-6.72	-2.99	-0.44	-1.76	-0.62	-1.56	0.06	-2.23	-1.62	0.12	-2.01	-3.35	-2.20	-1.17	3.49	0.48	
HCl	-10.46	-7.13	-3.41	-0.85	-2.18	-1.04	-1.98	-0.36	-2.65	-2.03	-0.29	-2.42	-3.76	-2.62	-1.59	-0.42	3.01	
SO ₂	-7.74	-4.41	-0.69	1.87	0.54	1.68	0.74	2.37	0.07	0.69	2.43	0.30	-1.04	0.11	1.13	2.30	2.72	
Low	900.	87.4	2.960	0.084	0.565	0.227	1.160	0.375	1.950	1.570	0.345	0.460	1.020	0.214	0.170	0.382	0.036	0.926
Center	961.	34.4	0.830	0.064	0.243	0.077	0.199	0.039	0.387	0.210	0.037	0.309	1.180	0.375	0.135	0.042	0.027	0.417
High	981.	15.5	0.287	0.020	0.064	0.017	0.060	0.018	0.181	0.063	0.016	0.110	1.610	0.316	0.093	0.005	0.001	0.363
clr(variance)	0.29	0.21	0.21	0.35	0.22	0.27	0.24	0.35	0.28	0.26	0.28	0.24	0.36	0.26	0.25	0.32	1.50	0.22

391 *3.2 Compositional linear trend as an alternative to MCE linear regression*

392 For all gases except CO₂, NO, and NO₂, the proportions decreased from the Low MCE
393 fire to the High MCE fire (Table 2, Table 3) which is consistent with previously reported
394 findings (Burling et al., 2010) suggesting the possibility of fitting a compositional linear trend
395 (Eq. (11)). The three possible starting compositions (**a**) for the linear trend and the estimated
396 perturbation vector (**p**) for each are contained in Table 3. The goodness of fit of the linear trend
397 to the data (determined by the first eigenvalue λ_1 as a percentage of the total variation) was 72.9,
398 77.5, and 50.1 percent for the High, Low and GM starting points, respectively. Of the three linear
399 trends, using the Low MCE composition as the starting point produced the smallest absolute
400 errors, lowest RMSE, and highest correlation between the observed and predicted values for 14
401 of the 18 gases (Table 4). While Low MCE produced the lowest mean bias (NMB) for 8 of the
402 gases and GM for 6 gases, NMB was similar for several gases for all three linear trends. Using
403 the GM as the starting point provided a better fit for NO₂, HONO and HCl. There was no
404 correlation between observed and predicted values for C₂H₂ from any of the three linear trends.
405 The observed and predicted values for NO₂ and HCl were negatively correlated for the Low
406 MCE trend.

407 When compared to the fitted ordinary linear regressions for each gas, the Low MCE
408 compositional trend had smaller errors (NMAE) for 12 of the 18 gases, lower RMSE for 8 of the
409 18 and higher correlation (r) for 13 of the 18 gases (Table 5). Overall, the geometric mean
410 NMAE for the CLT (0.26) was less than LR (0.30) indicating the linear trend estimates had less
411 error than the linear regression estimates; however, the CLT was negatively biased. Bias for
412 linear regression was 0 in all cases because the residuals ($\hat{y}_i - y_i$) sum to 0 for every linear

413 regression with an intercept term (Draper & Smith, 1981). Mean RMSE for the CLT and LR
414 were equal. The correlations between observed and estimated values for most of the trace gases
415 were similar between the linear trend and the linear regression models. For the linear trend,
416 correlation between observed and predicted values was not significant for C₂H₂ and NO; for
417 linear regression there was no significant correlation between observed and predicted values for
418 NO₂ and HCl. In some cases (such as HONO), the EF was fairly constant (Figure 1). For 9 of the
419 16 gases, correlation for the CLT was larger than for the LR. For the overall measures, the
420 coefficient of determination R_{CLT}^2 for the Low MCE linear trend (0.283) was lower than the
421 comparable measure R_{LR}^2 for the multivariate linear regression (0.933). It is interesting to note
422 that R_{CLT}^2 GM linear trend was 0.501. Because R_{CLT}^2 is a measure of the entire composition
423 projected onto the first principal component, parts of the composition (gases) more strongly
424 associated with other principal components would contribute to the lack of fit of the linear trend.
425 Preliminary analysis of the data using a biplot (Aitchison & Greenacre, 2002) suggested that HCl
426 was not strongly associated with the first principal component (not shown) which decreased the
427 amount of variability that the linear trend would account for thus reducing its predictive ability.
428 Recall that the clr-variance for HCl was nearly 25% of the total variance. The fitted values of
429 HCL by both the linear trend and the linear regression were relatively constant (Figure 1). The
430 $RMSE_{CLT}$ ranged from 0.426 to 0.511 for the three starting points which was much smaller than
431 $RMSE_{LR}$ (2.658). It is important to note that because compositional data are restricted to positive
432 upper orthant, predictions from the linear trend were always positive unlike predictions from the
433 linear regression. The predictions from the linear regression in Figure 1 are the fitted values, not
434 predictions made outside the range of the data. The fitted linear regressions for 6 of the 18 gases

435 produced values below zero. Scatterplots for all 18 gases are available in the supplementary
436 information. Generally, the CLT performed equal to or superior to the LR based on MCE. This
437 coupled with the fact that the compositional nature of emissions data were analyzed using
438 techniques appropriate to the type of data indicates the value of this analytical approach.

439 The data set used to demonstrate this technique was one that was readily available to the
440 authors. There are at several compilations of emission factor data that could be used to explore if
441 smoke composition changes linearly as efficiency of a fire changes (Akagi et al., 2011; Lincoln
442 et al., 2014; Yokelson et al., 2013). If a linear trend can be successfully fit for a larger data set
443 producing better goodness of fit measures, such a linear trend could be used to reliably estimate
444 emissions of gases not typically measured if the log-ratio variance of the parts is relatively low.

445 3.3 Testing the effects of fuel type on compositional data

446 In the original report (Burling et al., 2010), effects of fuel type on subsets of the
447 emissions were inferred from bar plots and error bars, but no formal hypothesis testing was
448 presented. The fuel types were representative of major local vegetation types in the southwestern
449 and southeastern U.S. The pine litter fuel type was the sole type composed of only dead pine
450 needles (*Pinus* spp.) and branches. All other fuel types included live foliage and branches in
451 addition to dead fuels. In the present study compositional balances 1 to 7 were designed to test
452 meaningful observations reported in Burling et al. (2010); whereas balances 8-17 were necessary
453 to obtain the full projection of the compositions from the simplex into real-valued ilr coordinates
454 but are not defined according to any particular scientific relevance (see supplemental data). The
455 intercept term, which is the mean for the 1-year rough fuel type due to ANOVA
456 parameterization, was statistically significant for 5 of the 7 balances of interest (Table 6). For the

457 significant intercepts, a positive value indicated that the numerator of the balance was on average
458 relatively larger than the denominator, while a negative value indicated it was relatively smaller.
459 For example, there was relatively less N compared to the other compounds (hydrocarbons, C
460 oxides, etc.; balance 1) but relatively more NO_x than other N compounds (balance 2) for the 1-
461 year rough fuel type. The estimated effect for a fuel type is the sum of the intercept and the fuel
462 type value. Thus the estimate of balance 1 for pine litter was -2.02 (-1.18 + -0.84); because the
463 fuel type value was significant, the composition of the emissions for pine litter had relatively
464 even less N compared to other compounds; similarly the oak savanna and woodland fuel types
465 had relatively more N compared to other compounds since the balance estimate was close to -0.2
466 for these fuels. For balance 1, the relative amount of N versus the other compounds for the other
467 fuel types was not significantly different from the 1 yr rough. In addition to the smoke containing
468 relatively more NO_x compared to the other N compounds (balance 2 intercept), eight of the
469 southwestern fuel types had relatively more NO_x compared to other N compounds than five of
470 the six southeastern fuel types. Not surprisingly, there were relatively more C oxides than
471 organic C compounds (balance 5). We observed CH₄ in relatively higher quantities compared to
472 the non-methane organic compounds (NMOC) (balance 6). While overall NMHC and OVOC
473 relative abundances were statistically comparable for the 1-year fuel type (balance 7 is not
474 significantly different from zero), a significant negative difference with respect to this baseline
475 was concluded for seven of the other fuel types, suggesting that relatively more OVOC
476 compared to NMHC was observed on average for those fuel types. The relative amount of NH₃
477 to NO_x (balance 3) did not differ significantly between all fuel types except for the oak savanna
478 fuel type. The overall amounts of HCl and SO₂ observed were much smaller in comparison to the

479 quantities of C compounds (balance 4); however, eight of the fuel types significantly reduced
 480 this difference in relative amounts.

481
 482 **Table 3. Starting point compositions (a) in original units (g kg⁻¹) and estimated perturbation**
 483 **vectors (p) for a compositional linear trend fit to a data set of smoke emissions from**
 484 **wildland fuels. The starting points after closure are contained in Table 2.**

485

Gas	Starting point (a)			Perturbation (p)		
	Low MCE (0.911)	Center	High MCE (0.984)	Low MCE	Center	High MCE
CO ₂	1584.6780	1739.8798	1745.3486	0.0716	0.0572	0.0722
CO	153.7918	62.2174	27.5268	0.0552	0.0558	0.0569
CH ₄	5.2066	1.5030	0.5105	0.0500	0.0521	0.0525
C ₂ H ₂	0.1473	0.1167	0.0358	0.0654	0.0583	0.0510
C ₂ H ₄	0.9946	0.4395	0.1144	0.0553	0.0503	0.0491
C ₃ H ₆	0.3993	0.1402	0.0299	0.0515	0.0472	0.0464
CH ₃ OH	2.0335	0.3601	0.1060	0.0434	0.0472	0.0506
HCOOH	0.6595	0.0708	0.0317	0.0380	0.0442	0.0572
CH ₃ COOH	3.4240	0.7000	0.3222	0.0448	0.0457	0.0574
HCHO	2.7553	0.3799	0.1128	0.0408	0.0471	0.0507
C ₄ H ₄ O	0.6071	0.0666	0.0282	0.0387	0.0465	0.0563
NH ₃	0.8104	0.5600	0.1948	0.0627	0.0539	0.0534
NO	1.7903	2.1428	2.8557	0.0736	0.0572	0.0785
NO ₂	0.3762	0.6791	0.5613	0.0795	0.0548	0.0680
HONO	0.2986	0.2439	0.1652	0.0651	0.0503	0.0651
HCN	0.6733	0.0754	0.0086	0.0386	0.0468	0.0389
HCl	0.0631	0.0497	0.0025	0.0689	0.1327	0.0273
SO ₂	1.6302	0.7546	0.6450	0.0569	0.0528	0.0686

486

487

488 **Table 4. Ordinary measures of fit based on observed and predicted emission factors for**
 489 **compositional linear trends that started at the High, Low or geometric mean (GM) value of**
 490 **MCE for gases associated with smoke from wildland fire. Highlighted values indicate the**
 491 **best value for each measure by gas.**

Gas	NMB			NMAE ¹			RMSE			r		
	High	Low	GM	High	Low	GM	High	Low	GM	High	Low	GM
CO ₂	0.00	0.00	0.00	0.01	0.01	0.01	26.16	16.65	26.60	0.94	0.98	0.94
CO	-0.07	0.04	-0.05	0.26	0.20	0.24	22.35	16.26	22.77	0.38	0.78	0.08 ^N
CH ₄	-0.15	-0.04	-0.14	0.40	0.30	0.42	1.08	0.68	1.10	0.32	0.79	0.24
C ₂ H ₂	-0.23	-0.24	-0.24	0.52	0.53	0.54	0.15	0.15	0.15	0.16 ^N	0.12 ^N	-0.10 ^N
C ₂ H ₄	-0.21	-0.19	-0.18	0.50	0.37	0.47	0.49	0.42	0.47	0.17 ^N	0.58	0.30
C ₃ H ₆	-0.28	-0.26	-0.23	0.59	0.41	0.55	0.17	0.14	0.17	0.24	0.74	0.32
CH ₃ OH	-0.29	-0.12	-0.24	0.63	0.27	0.55	0.51	0.23	0.50	0.25	0.92	0.29
HCOOH	-0.40	-0.11	-0.32	0.73	0.28	0.68	0.14	0.06	0.14	0.17 ^N	0.92	0.27
CH ₃ COOH	-0.33	-0.21	-0.26	0.67	0.34	0.60	1.11	0.66	1.08	0.20 ^N	0.87	0.28
HCHO	-0.31	-0.07	-0.27	0.65	0.26	0.59	0.58	0.24	0.56	0.19 ^N	0.91	0.32
C ₄ H ₄ O	-0.33	0.02	-0.27	0.63	0.23	0.56	0.12	0.03	0.12	0.22 ^N	0.96	0.27
NH ₃	-0.12	-0.12	-0.09	0.37	0.33	0.36	0.30	0.27	0.29	0.29	0.43	0.12 ^N
NO	0.00	-0.01	-0.02	0.17	0.16	0.18	0.48	0.47	0.50	0.31	0.18 ^N	-0.21 ^N
NO ₂	-0.08	-0.17	-0.07	0.32	0.37	0.32	0.32	0.39	0.31	0.18 ^N	-0.43	0.21 ^N
HONO	-0.16	-0.16	-0.09	0.41	0.35	0.35	0.16	0.14	0.14	-0.02 ^N	0.58	0.41
HCN	-0.38	-0.14	-0.37	0.73	0.36	0.68	0.17	0.08	0.17	0.27	0.92	0.28
HCl	-0.17	-0.47	-0.02	0.42	0.77	0.35	0.08	0.14	0.06	0.85	-0.32	0.90
SO ₂	-0.05	-0.01	-0.05	0.27	0.20	0.28	0.31	0.20	0.30	-0.03 ^N	0.75	0.25

492 1. NMB is normalized mean bias, NMAE is normalized mean average error, RMSE is root
 493 mean squared error, r is Pearson correlation coefficient – N indicates that r is not significantly
 494 different from 0 at 5% significance level based on t-test.

$$\text{NMB} = \frac{1}{n} \sum_{i=1}^n (\hat{y}_i - y_i) / \bar{y}$$

$$495 \quad \text{NMAE} = \frac{1}{n} \sum_{i=1}^n |\hat{y}_i - y_i| / \bar{y}$$

$$\text{RMSE} = \sqrt{\frac{1}{n} \sum_{i=1}^n (\hat{y}_i - y_i)^2}$$

496 where y_i , \hat{y}_i , \bar{y} are observed, predicted, and mean emission factor (g/kg); n is number of
 497 observations.

498

499 **Table 5. Measures of goodness of fit¹ of estimates for the Low MCE compositional linear**
 500 **trend (CLT) and linear regression (LR) with observed smoke emissions from wildland fire.**

	NMAE		NMB	RMSE		r	
	CLT	LR	CLT	CLT	LR	CLT	LR
CO ₂	0.01		0.00	16.65		0.98	
CO	0.20		0.04	16.26		0.78	
CH ₄	0.30	0.30	-0.04	0.68	0.66	0.79	0.80
C ₂ H ₂	0.53	0.55	-0.24	0.15	0.14	0.12 ^N	0.35
C ₂ H ₄	0.37	0.34	-0.19	0.42	0.39	0.58	0.59
C ₃ H ₆	0.41	0.45	-0.26	0.14	0.12	0.74	0.69
CH ₃ OH	0.27	0.41	-0.12	0.23	0.26	0.92	0.86
HCOOH	0.28	0.55	-0.11	0.06	0.08	0.92	0.81
CH ₃ COOH	0.34	0.50	-0.21	0.66	0.70	0.87	0.76
HCHO	0.26	0.42	-0.07	0.24	0.30	0.91	0.85
C ₄ H ₄ O	0.23	0.52	0.02	0.03	0.06	0.96	0.84
NH ₃	0.33	0.32	-0.12	0.27	0.25	0.43	0.47
NO	0.16	0.15	-0.01	0.47	0.45	0.18 ^N	0.35
NO ₂	0.37	0.31	-0.17	0.39	0.31	-0.43	0.24 ^N
HONO	0.35	0.41	-0.16	0.14	0.14	0.58	0.34
HCN	0.36	0.51	-0.14	0.08	0.09	0.92	0.83
HCl	0.77	0.82	-0.47	0.14	0.13	-0.32	0.04 ^N
SO ₂	0.20	0.21	-0.01	0.20	0.21	0.75	0.73
Mean	0.26	0.30	-0.13	0.33	0.33		

501 1. NMB is normalized mean bias, NMAE is normalized mean average error, RMSE is root
 502 mean squared error, r is Pearson correlation coefficient – N indicates that r is not
 503 significantly different from 0 at probability = 0.05 based on t-test.

$$\text{NMB} = \frac{1}{n} \sum_{i=1}^n (\hat{y}_i - y_i) / \bar{y}$$

504
$$\text{NMAE} = \frac{1}{n} \sum_{i=1}^n |\hat{y}_i - y_i| / \bar{y}$$

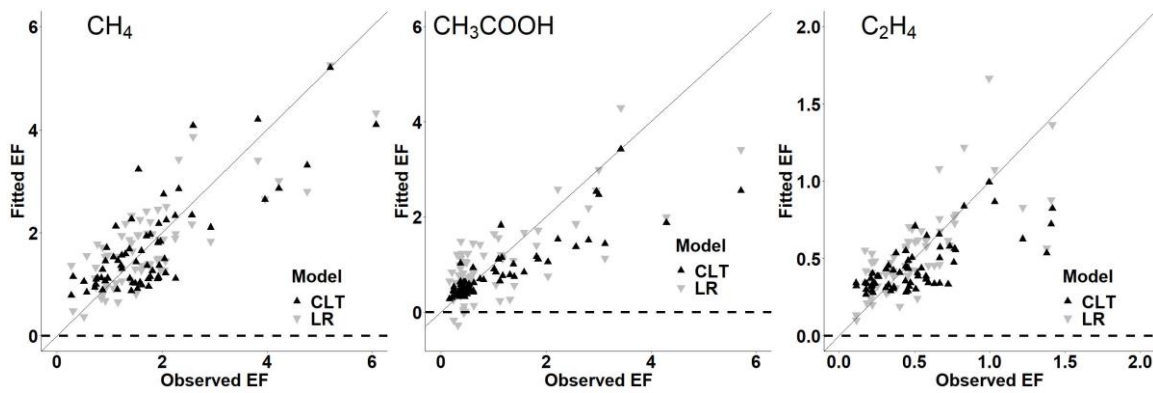
$$\text{RMSE} = \sqrt{\frac{1}{n} \sum_{i=1}^n (\hat{y}_i - y_i)^2}$$

505 where y_i , \hat{y}_i , \bar{y} are observed, predicted, and mean emission factor (g/kg); n is number of
 506 observations. Mean value of NMAE calculated as geometric mean, mean RMSE calculated
 507 square root of mean of squared RMSE.

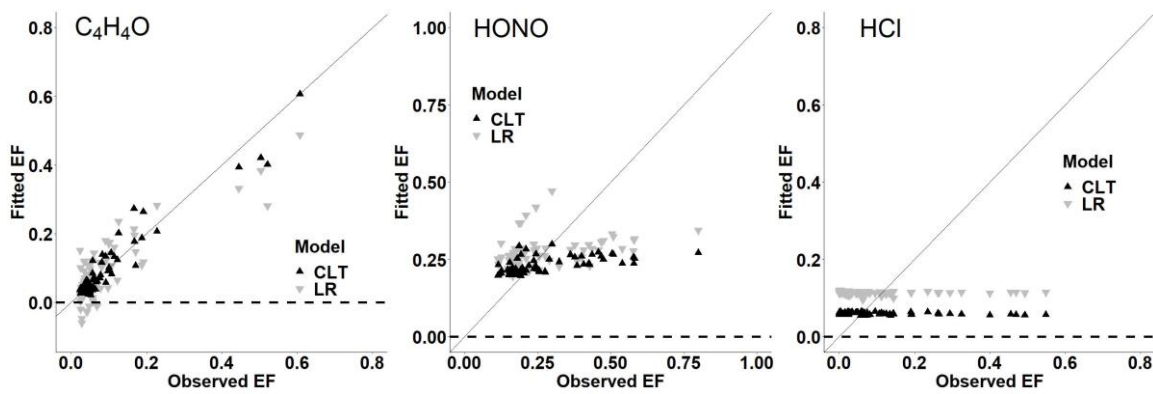
508

509

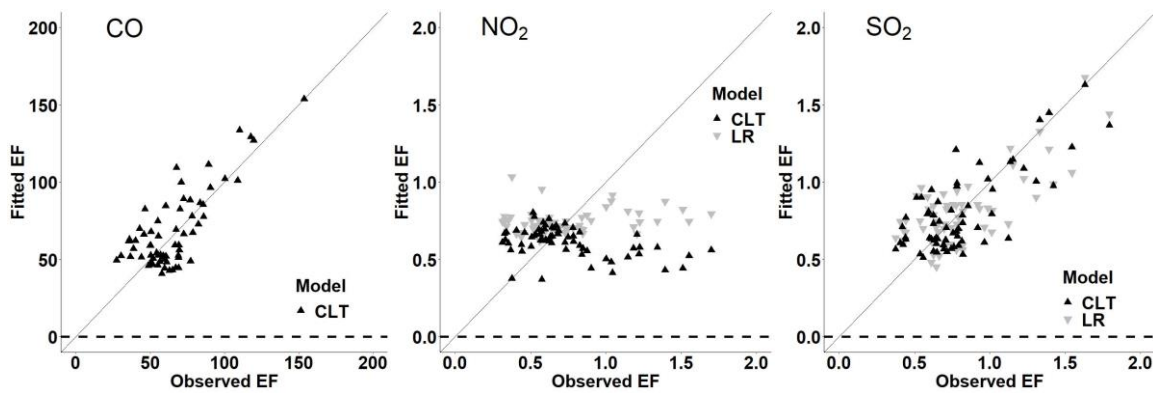
510



511



512



513

514

515 **Figure 1. Comparison of observed emission factors (EF) for several wildland fire gases with**
 516 **fitted EF from a compositional linear trend (CLT) and a linear regression (LR) using**
 517 **modified combustion efficiency as the predictor variable.**

518

519 **Table 6. Significance of mean differences in compositional balances of smoke emissions from wildland fire according to fuel**
 520 **type. * = p-value < 0.05. Significant differences are shown in grey text. Dark grey denotes the balances of interest, light grey**
 521 **denotes the other balances. P-values adjusted to control for false discovery rate.**

ID	Balance	Intercept (1 year rough) ¹	2 year rough	California sagebrush	Ceanothus	Chamise/scrub oak	Coastal sage scrub	Chipped understory hardwood	Pine litter	Manzanita	Maritime chaparral	Masticated mesquite	Oak savanna	Oak woodland	Pecosin	Understory hardwood
1	N vs other	-1.18*	0.12	-0.08	0.25	0.02	-0.01	0.08	-0.84*	0.15	0.10	0.52	0.97*	0.99*	-0.39	0.39
2	NO _x vs other N	1.17*	0.02	0.48	1.06*	0.70*	0.58*	0.99*	-0.20	1.22*	0.68*	1.01*	1.61*	0.88*	0.53	0.50
3	NH ₃ vs NO _x	-0.34	-0.04	0.08	-0.55	-0.44	-0.11	-0.43	0.09	-0.55	0.02	-0.26	-0.94*	-0.23	-0.45	-0.39
4	HCl & SO ₂ vs C	-3.61*	0.59	2.51*	2.10*	0.79	1.96*	1.80*	0.89	2.67*	2.97*	2.26*	0.86	0.15	1.94*	0.42
5	C oxide vs OC	8.17*	0.01	1.01*	1.10*	0.83*	1.34*	1.57*	-0.23	1.83*	1.20*	1.25*	1.75*	1.30*	0.44	0.59
6	CH ₄ vs NMOC	1.65*	0.04	0.42*	-0.01	-0.02	0.58*	0.77*	-0.14	0.09	0.55*	0.63*	0.27	0.35*	-0.15	-0.14
7	NMHC vs OVOC	0.40	-0.90*	0.39	-0.97*	-0.74*	0.55*	-0.27	-1.90*	-0.48	0.37	-0.47	-0.95*	-0.06	-1.64*	-1.27*
8	Alkene vs alkyne	1.08*	-0.06	-0.26	-0.18	0.03	-0.23	-0.11	0.05	-0.16	-0.12	0.00	0.04	-0.02	-0.06	-0.04
9	Furan vs OVOC	-1.80*	0.07	0.54*	0.38	0.45*	0.44*	0.57*	0.74*	0.96*	0.67*	0.24	0.59*	0.70*	0.20	0.37
10	Formaldehyde vs OVOC	0.44*	-0.28	-0.02	-0.15	-0.08	0.07	-0.05	-0.17	-0.01	0.04	-0.18	-0.37*	-0.17	-0.22	-0.12
11	HCl vs SO ₂	-2.99*	0.28	1.84*	2.12*	0.78	1.28*	1.52*	0.96	2.05*	2.52*	1.37*	-0.61	-0.90	1.82*	-0.08
12	NO vs NO ₂	0.48*	-0.04	0.57*	0.17	0.48*	0.70*	0.08	0.07	0.54*	0.50*	0.37*	0.65*	0.76*	-0.59*	0.04
13	CH ₃ vs HCOOH	1.47*	0.12	0.30	-0.13	0.07	0.26	0.28	0.02	-0.03	0.46	0.37	-0.08	0.27	-0.10	0.12
14	CH ₃ COOH vs CH ₃ OH	-0.53*	-0.06	0.24*	-0.04	0.07	0.20	0.25*	0.11	0.05	0.18	0.25*	-0.19	0.11	-0.28*	-0.11
15	HONO vs HCN	0.70*	-0.38	0.19	0.62*	0.73*	0.05	0.19	-1.40*	0.48*	-0.12	-0.13	0.82*	0.30	0.30	0.35
16	CO vs CO ₂	-2.20*	0.08	-0.11	-0.15	-0.05	-0.07*	-0.34*	0.37	-0.16*	-0.22*	-0.25*	-0.59*	-0.46*	-0.24*	-0.26*
17	Acetylene vs Propene	-0.18	-0.40	0.60	0.19	-0.33*	1.14	-0.18	-0.70	0.52	-0.11	0.10	0.11	-0.30	-0.18	-0.24*

522 1. Standard ANOVA parameterization on balance ilr coordinates—the intercept term estimates the mean of the 1 year rough fuel

523 type and the value shown for the other types is the difference between the fuel type mean and the intercept (1yr fuel mean).

524

525 **4 Conclusions**

526 Smoke emissions data are inherently multivariate and relative in nature. While this has
527 been recognized for many years, the statistical techniques commonly used to analyze the data
528 ignore these features. This not only applies to the composition of the emissions, but also to the
529 different fuel types which burn to produce the emissions. Since emissions and fuel composition
530 represent parts of a whole, the measured values of the individual parts (elements, chemical
531 species, fuel component, etc.) are intrinsically not independent from each other. The measured
532 values are relative and are only meaningful in relation to each other. Such constraints violate
533 many of the underlying assumptions of ordinary statistical methods. Alternatively, compositional
534 data analysis as a well-developed body of statistical methodology provides models and methods
535 equivalent to traditional ones yet accounts for these special constraining features of relative data.
536 The approach has been used for decades to analyze analogous types of data in the geosciences
537 (Buccianti et al., 2006) and, more recently, in other disparate areas such as molecular biology to
538 analyze sequencing data (Quinn et al., 2018) or physical activity epidemiology for the analysis of
539 daily time-use patterns (Chastin et al., 2015; McGregor et al., 2019). While the statistical theory
540 may be unfamiliar and not typically taught in most statistics courses, recent publications and
541 software have made the use of these techniques both feasible and accessible.

542 The expression of emissions data as ratio data has long been reported. Even in this early
543 work, conversion of the composition of emissions between different units by simple
544 multiplication was presented, reinforcing the idea that emissions data form an equivalence class.
545 Transformation of data using the arc-sine and square root transformations for count data to
546 enable use of the normal distribution or to stabilize variance in linear regression and the log-odds

547 transformation used in logistic regression are familiar statistical techniques routinely used in the
548 atmospheric sciences and other fields. Linear transformation of data is used to code data to
549 simplify analysis for a variety of statistical calculations. The compositional data approach based
550 on log-ratio coordinates essentially maps the data onto the ordinary real space so that familiar
551 statistical techniques can be appropriately applied. This approach matches analysis techniques to
552 the data type thus reducing the possibility of the reporting of spurious results that may or may
553 not reflect the underlying relationships.

554 The linear regression approach as it has been typically applied uses one portion of the
555 composition (expressed as MCE) to predict other parts of the composition, which ignores the
556 intrinsic interplay between smoke emissions and can produce predictions beyond the domain of
557 their possible values, e.g. negative values. The compositional data analysis approach recognizes
558 the inherently positive-valued nature of the data thus eliminating the need for an analyst to
559 ignore or discount when a fitted model produces negative values. Robust methods have been
560 developed to allow inclusion of parts of a composition that are known to exist but fall below
561 detection limits thus permitting a more complete analysis. We have illustrated how the use of a
562 compositional linear trend to describe changes in the composition of smoke emissions as
563 combustion efficiency changed yielded predicted emission factors with error (difference between
564 observed and predicted) comparable to and, in some cases, superior to predictions from linear
565 regression models that used modified combustion efficiency as a predictor variable. Moreover,
566 the use of compositional balances to form log-ratios contrasting subsets of parts of interest
567 enabled the use of analysis of variance and hypothesis testing to examine differences in
568 meaningful trade-offs between smoke components with more formal rigor than was previously
569 presented by respecting the very relative nature of the data as derived from underlying natural

570 laws like conservation of mass. We have definitively shown that fuel type affected several
571 different ratios of groups of emissions and are assured that the results are not an artifact of the
572 analysis which can then be used to make various inferences and decisions. Near the end of the
573 article by Burling et al. (2010), there is discussion and hypothesis formation about the impacts of
574 wildland fuel management activities and influence of ocean proximity on the composition of
575 observed emissions. These impacts and hypotheses could be rigorously tested with the
576 techniques presented here. More complex analyses of log-ratios of gas pairs or groupings as
577 functions of external fire behavior variables such fire intensity (heat release rate) and flame
578 residence time are possible. More rigorous time series and spatial analysis to examine aging
579 smoke composition within the smoke plume and in response to atmospheric processes are
580 possible with compositional data. It is our view and recommendation that future analysis of the
581 composition of smoke emissions and other mixtures of atmospheric pollutants as well as general
582 atmospheric composition should consider the use of compositional data analysis methods to
583 provide more statistically rigorous and consistent results.

584 **Acknowledgments, Samples, and Data**

585 The data used in this paper resulted from projects the DOD/DOE/EPA Strategic
586 Environmental Research and Development Program projects RC-1648 and 1649. The senior
587 author appreciates the guidance and R scripts provided by Prof. Girty at San Diego State
588 University to estimate linear trends by perturbation. J. P.-A. was supported by the Spanish
589 Ministry of Science, Innovation and Universities under the project CODAMET (RTI2018-
590 095518-B-C21, 2019-2021). The data used in this study have been previously published and are
591 available in the original publications. DRW conceived the initial manuscript (70 percent) and
592 performed the bulk of the data analysis. JPA provided statistical guidance and compositional data

593 expertise and contributed 20 percent of the manuscript. TJJ and HJ were extensively involved in
594 the study that provided the data. TJJ provide smoke emissions expertise and HJ provided
595 combustion expertise. The authors declare that they have no conflict of interest. The use of trade
596 or firm names in this publication is for reader information and does not imply endorsement by
597 the U.S. Department of Agriculture of any product or service.

598 **References**

- 599 Aitchison, J. (1982). The statistical analysis of compositional data. *Journal of the Royal*
600 *Statistical Society. Series B (Methodological)*, 44(2), 139–177.
- 601 Aitchison, J. (1986). *The statistical analysis of compositional data*. London ; New York:
602 Chapman and Hall.
- 603 Aitchison, J. (2003). A concise guide to compositional data analysis. In *CDA Workshop, Girona*.
- 604 Aitchison, J., & Greenacre, M. (2002). Biplots of compositional data. *Journal of the Royal*
605 *Statistical Society: Series C (Applied Statistics)*, 51(4), 375–392.
606 <https://doi.org/10.1111/1467-9876.00275>
- 607 Akagi, S. K., Yokelson, R. J., Wiedinmyer, C., Alvarado, M. J., Reid, J. S., Karl, T., et al.
608 (2011). Emission factors for open and domestic biomass burning for use in atmospheric
609 models. *Atmospheric Chemistry and Physics*, 11(9), 4039–4072.
610 <https://doi.org/10.5194/acp-11-4039-2011>
- 611 Amaral, S. S., de Carvalho, J. A., Jr., Costa, M. A. M., Neto, T. G. S., Dellani, R., & Leite, L. H.
612 S. (2014). Comparative study for hardwood and softwood forest biomass: Chemical
613 characterization, combustion phases and gas and particulate matter emissions.
614 *Bioresource Technology*, 164, 55–63. <https://doi.org/10.1016/j.biortech.2014.04.060>

- 615 Anderson, G. K., Sandberg, D. V., & Norheim, R.A. (2004, January). Fire Emission Production
616 Simulator (FEPS) User's Guide 1.0. USDA Forest Service, Pacific Northwest Research
617 Station.
- 618 Andreae, M. O., & Merlet, P. (2001). Emission of trace gases and aerosols from biomass
619 burning. *Global Biogeochemical Cycles*, *15*(4), 955–966.
620 <https://doi.org/10.1029/2000GB001382>
- 621 Bandeen-Roche, K. (1994). Resolution of additive mixtures into source components and
622 contributions: a compositional approach. *Journal of the American Statistical Association*,
623 *89*(428), 1450–1458. <https://doi.org/10.1080/01621459.1994.10476883>
- 624 Barcelo-Vidal, C., & Martín-Fernández, J.-A. (2016). The Mathematics of Compositional
625 Analysis. *Austrian Journal of Statistics*, *45*(4), 57. <https://doi.org/10.17713/ajs.v45i4.142>
- 626 Barceló-Vidal, C., Martín-Fernández, J. A., & Pawlowsky-Glahn, V. (2001). Mathematical
627 foundations of compositional data analysis. In G. Ross (Ed.), *Proceedings of IAMG'01*
628 (Vol. CD-ROM, p. 20). Cancun, MX: International Association for Mathematical
629 Geosciences. Retrieved from http://ima.udg.edu/~barcelo/index_archivos/Cancun.pdf
- 630 Benjamini, Y., & Hochberg, Y. (1995). Controlling the false discovery rate: a practical and
631 powerful approach to multiple testing. *Journal of the Royal Statistical Society. Series B*
632 (*Methodological*), *57*(1), 289–300.
- 633 Billheimer, D. (2001). Compositional receptor modeling. *Environmetrics*, *12*(5), 451–467.
634 <https://doi.org/10.1002/env.472>
- 635 van den Boogaart, K. G., & Tolosana-Delgado, R. (2013). *Analyzing compositional data with R*.
636 Heidelberg: Springer.

- 637 Bucciante, A., & Pawlowsky-Glahn, V. (2006). Statistical evaluation of compositional changes in
638 volcanic gas chemistry: a case study. *Stochastic Environmental Research and Risk*
639 *Assessment*, 21(1), 25–33. <https://doi.org/10.1007/s00477-006-0041-x>
- 640 Bucciante, A., Mateu-Figueras, G., & Pawlowsky-Glahn, V. (Eds.). (2006). *Compositional data*
641 *analysis in the geosciences: from theory to practice*. London: The Geological Society.
- 642 Burling, I. R., Yokelson, R. J., Griffith, D. W. T., Johnson, T. J., Veres, P., Roberts, J. M., et al.
643 (2010). Laboratory measurements of trace gas emissions from biomass burning of fuel
644 types from the southeastern and southwestern United States. *Atmospheric Chemistry and*
645 *Physics*, 10(22), 11115–11130. <https://doi.org/10.5194/acp-10-11115-2010>
- 646 Byram, G. M. (1957). Some principles of combustion and their significance in forest fire
647 behavior. *Fire Control Notes*, 18(2), 47–57.
- 648 Byram, G. M. (1959). Combustion of forest fuels. In K. P. Davis (Ed.), *Forest Fire: Control and*
649 *Use* (1st ed., pp. 61–89). New York: McGraw-Hill.
- 650 Carslaw, D. C. (2015). *The openair manual— open-source tools for analysing air pollution data*
651 (Manual No. 1.1-4) (p. 287). London, UK: King’s College. Retrieved from
652 http://www.openair-project.org/PDF/OpenAir_Manual.pdf
- 653 Carslaw, D. C., & Ropkins, K. (2012). openair — An R package for air quality data analysis.
654 *Environmental Modelling & Software*, 27–28, 52–61.
655 <https://doi.org/10.1016/j.envsoft.2011.09.008>
- 656 Cayuela-Sánchez, J. A., Palarea-Albaladejo, J., García-Martín, J. F., & Pérez-Camino, M. del C.
657 (2019). Olive oil nutritional labeling by using Vis/NIR spectroscopy and compositional

- 658 statistical methods. *Innovative Food Science & Emerging Technologies*, 51, 139–147.
659 <https://doi.org/10.1016/j.ifset.2018.05.018>
- 660 Chang-Graham, A. L., Profeta, L. T. M., Johnson, T. J., Yokelson, R. J., Laskin, A., & Laskin, J.
661 (2011). Case study of water-soluble metal containing organic constituents of biomass
662 burning aerosol. *Environmental Science & Technology*, 45(4), 1257–1263.
663 <https://doi.org/10.1021/es103010j>
- 664 Chastin, S. F. M., Palarea-Albaladejo, J., Dontje, M. L., & Skelton, D. A. (2015). Combined
665 Effects of Time Spent in Physical Activity, Sedentary Behaviors and Sleep on Obesity
666 and Cardio-Metabolic Health Markers: A Novel Compositional Data Analysis Approach.
667 *PLOS ONE*, 10(10), e0139984. <https://doi.org/10.1371/journal.pone.0139984>
- 668 Crutzen, P. J., & Brauch, H. G. (Eds.). (2016). *Paul J. Crutzen: a pioneer on atmospheric*
669 *chemistry and climate in the anthropocene*. Zürich: Springer.
- 670 Darley, E. F., Burleson, F. R., Mateer, E. H., Middleton, J. T., & Osterli, V. P. (1966).
671 Contribution of Burning of Agricultural Wastes to Photochemical Air Pollution. *Journal*
672 *of the Air Pollution Control Association*, 16(12), 685–690.
673 <https://doi.org/10.1080/00022470.1966.10468533>
- 674 Di Blasi, C. (2008). Modeling chemical and physical processes of wood and biomass pyrolysis.
675 *Progress in Energy and Combustion Science*, 34(1), 47–90.
676 <https://doi.org/10.1016/j.pecs.2006.12.001>
- 677 Draper, N. R., & Smith, H. (1981). *Applied regression analysis* (2d ed). New York: Wiley.
- 678 Egozcue, J.J. (2009). Reply to “On the Harker Variation Diagrams; ...” by J.A. Cortés.
679 *Mathematical Geosciences*, 41(7), 829–834. <https://doi.org/10.1007/s11004-009-9238-0>

- 680 Egozcue, J.J., & Pawlowsky-Glahn, V. (2005). Groups of parts and their balances in
681 compositional data analysis. *Mathematical Geology*, 37(7), 795–828.
682 <https://doi.org/10.1007/s11004-005-7381-9>
- 683 Egozcue, J.J., & Pawlowsky-Glahn, V. (2011). Basic Concepts and Procedures. In V.
684 Pawlowsky-Glahn & A. Buccianti (Eds.), *Compositional Data Analysis* (pp. 12–28).
685 Chichester, UK: John Wiley & Sons, Ltd. <https://doi.org/10.1002/9781119976462.ch2>
- 686 Egozcue, J.J., Lovell, D., & Pawlowsky-Glahn, V. (2014). Testing compositional association. In
687 K. Hron, P. Filzmoser, & M. Templ (Eds.), *Proceedings of the 5th International*
688 *Workshop on Compositional Data Analysis* (pp. 28–36). Vorau, Austria. Retrieved from
689 <http://www.statistik.tuwien.ac.at/CoDaWork/CoDaWork2013Proceedings.pdf>
- 690 Egozcue, J.J., Pawlowsky-Glahn, V., & Gloor, G. B. (2018). Linear Association in
691 Compositional Data Analysis. *Austrian Journal of Statistics*, 47(1), 3.
692 <https://doi.org/10.17713/ajs.v47i1.689>
- 693 von Eynatten, H. (2004). Statistical modelling of compositional trends in sediments. *Sedimentary*
694 *Geology*, 171(1–4), 79–89. <https://doi.org/10.1016/j.sedgeo.2004.05.011>
- 695 von Eynatten, H., Barceló-Vidal, C., & Pawlowsky-Glahn, V. (2003). Modelling compositional
696 change: the example of chemical weathering of granitoid rocks. *Mathematical Geology*,
697 35(3), 231–251. <https://doi.org/10.1023/A:1023835513705>
- 698 Ferek, R. J., Reid, J. S., Hobbs, P. V., Blake, D. R., & Lioussé, C. (1998). Emission factors of
699 hydrocarbons, halocarbons, trace gases and particles from biomass burning in Brazil.
700 *Journal of Geophysical Research: Atmospheres*, 103(D24), 32107–32118.
701 <https://doi.org/10.1029/98JD00692>

- 702 Ferguson, S. C., Dahale, A., Shotorban, B., Mahalingam, S., & Weise, D. R. (2013). The role of
703 moisture on combustion of pyrolysis gases in wildland fires. *Combustion Science and*
704 *Technology*, 185, 435–453. <https://doi.org/10.1080/00102202.2012.726666>
- 705 Filzmoser, P., Hron, K., & Templ, M. (2018). *Applied compositional data analysis: with worked*
706 *examples in R*. New York, NY: Springer Berlin Heidelberg.
- 707 Fox, J., & Weisberg, S. (2018, September 21). Multivariate linear models in R: an appendix to
708 “An R Companion to Applied Regression”, 3rd edition. Retrieved from
709 [https://socialsciences.mcmaster.ca/jfox/Books/Companion/appendices/Appendix-](https://socialsciences.mcmaster.ca/jfox/Books/Companion/appendices/Appendix-Multivariate-Linear-Models.pdf)
710 [Multivariate-Linear-Models.pdf](https://socialsciences.mcmaster.ca/jfox/Books/Companion/appendices/Appendix-Multivariate-Linear-Models.pdf)
- 711 Fox, J., & Weisberg, S. (2019). *An R companion to applied regression* (Third edition). Thousand
712 Oaks, California: Sage Publications, Inc.
- 713 Gerstle, R. W., & Kemnitz, D. A. (1967). Atmospheric Emissions from Open Burning. *Journal*
714 *of the Air Pollution Control Association*, 17(5), 324–327.
715 <https://doi.org/10.1080/00022470.1967.10468988>
- 716 Gilman, J. B., Lerner, B. M., Kuster, W. C., Goldan, P. D., Warneke, C., Veres, P. R., et al.
717 (2015). Biomass burning emissions and potential air quality impacts of volatile organic
718 compounds and other trace gases from fuels common in the US. *Atmospheric Chemistry*
719 *and Physics*, 15(24), 13915–13938. <https://doi.org/10.5194/acp-15-13915-2015>
- 720 Goode, J. G., Yokelson, R. J., Ward, D. E., Susott, R. A., Babbitt, R. E., Davies, M. A., & Hao,
721 W. M. (2000). Measurements of excess O₃, CO₂, CO, CH₄, C₂H₄, C₂H₂, HCN,
722 NO, NH₃, HCOOH, CH₃COOH, HCHO, and CH₃OH in 1997 Alaskan biomass

- 723 burning plumes by airborne Fourier transform infrared spectroscopy (AFTIR). *Journal of*
724 *Geophysical Research*, 105(D17), 22147. <https://doi.org/10.1029/2000JD900287>
- 725 Graybill, F. A. (2002). *Matrices with applications in statistics*. Belmont: Duxbury.
- 726 Hosseini, S., Li, Q., Cocker, D., Weise, D., Miller, A., Shrivastava, M., et al. (2010). Particle size
727 distributions from laboratory-scale biomass fires using fast response instruments.
728 *Atmospheric Chemistry and Physics*, 10(16), 8065–8076. [https://doi.org/10.5194/acp-10-](https://doi.org/10.5194/acp-10-8065-2010)
729 8065-2010
- 730 Hosseini, S., Urbanski, S. P., Dixit, P., Qi, L., Burling, I. R., Yokelson, R. J., et al. (2013).
731 Laboratory characterization of PM emissions from combustion of wildland biomass fuels:
732 particle emissions from biomass burning. *Journal of Geophysical Research:*
733 *Atmospheres*, 118(17), 9914–9929. <https://doi.org/10.1002/jgrd.50481>
- 734 Hough, W. A. (1969). *Caloric value of some forest fuels of the southern United States* (Research
735 Note No. SE-120) (p. 6). Asheville, NC: USDA Forest Service, Southeastern Forest
736 Experiment Station. Retrieved from <http://www.treesearch.fs.fed.us/pubs/2778>
- 737 Janhäll, S., Andreae, M. O., & Pöschl, U. (2010). Biomass burning aerosol emissions from
738 vegetation fires: particle number and mass emission factors and size distributions.
739 *Atmospheric Chemistry and Physics*, 10(3), 1427–1439. [https://doi.org/10.5194/acp-10-](https://doi.org/10.5194/acp-10-1427-2010)
740 1427-2010
- 741 Jolly, W. M., Hintz, J., Linn, R. L., Kropp, R. C., Conrad, E. T., Parsons, R. A., & Winterkamp,
742 J. (2016). Seasonal variations in red pine (*Pinus resinosa*) and jack pine (*Pinus*
743 *banksiana*) foliar physio-chemistry and their potential influence on stand-scale wildland

- 744 fire behavior. *Forest Ecology and Management*, 373, 167–178.
745 <https://doi.org/10.1016/j.foreco.2016.04.005>
- 746 Lincoln, E., Hao, W., Weise, D. R., & Johnson, T. J. (2014). *Wildland fire emission factors*
747 *database* (Archived data No. RDS-2014-0012). Fort Collins, CO: USDA Forest Service
748 Research Data Archive. Retrieved from <http://dx.doi.org/10.2737/RDS-2014-0012>
- 749 Lobert, J. M., & Warnatz, J. (1993). 2 - Emissions from the combustion process in vegetation. In
750 P. J. Crutzen & J. G. Goldammer (Eds.), *Fire in the Environment: The Ecological*
751 *Atmospheric, and Climatic Importance of Vegetation Fires* (pp. 15–37). John Wiley &
752 Sons Ltd.
- 753 Lobert, J. M., Scharffe, D. H., Hao, W. M., & Crutzen, P. J. (1990). Importance of biomass
754 burning in the atmospheric budgets of nitrogen-containing gases. *Nature*, 346(6284),
755 552–554. <https://doi.org/10.1038/346552a0>
- 756 Lovell, D., Pawlowsky-Glahn, V., Egozcue, J. J., Marguerat, S., & Bähler, J. (2015).
757 Proportionality: A Valid Alternative to Correlation for Relative Data. *PLoS*
758 *Computational Biology*, 11(3), e1004075. <https://doi.org/10.1371/journal.pcbi.1004075>
- 759 Mardia, K. V., Kent, J. T., & Bibby, J. M. (1979). *Multivariate analysis*. London ; New York:
760 Academic Press.
- 761 Mateu-Figueras, G., Pawlowsky-Glahn, V., & Egozcue, J. J. (2011). The Principle of Working
762 on Coordinates. In V. Pawlowsky-Glahn & A. Buccianti (Eds.), *Compositional Data*
763 *Analysis* (pp. 31–42). Chichester, UK: John Wiley & Sons, Ltd.
764 <https://doi.org/10.1002/9781119976462.ch3>

- 765 May, A. A., McMeeking, G. R., Lee, T., Taylor, J. W., Craven, J. S., Burling, I., et al. (2014).
766 Aerosol emissions from prescribed fires in the United States: A synthesis of laboratory
767 and aircraft measurements: Aerosols from US prescribed fires. *Journal of Geophysical*
768 *Research: Atmospheres*, 119(20), 11,826-11,849. <https://doi.org/10.1002/2014JD021848>
- 769 McGregor, D., Palarea-Albaladejo, J., Dall, P., Hron, K., & Chastin, S. (2019). Cox regression
770 survival analysis with compositional covariates: Application to modelling mortality risk
771 from 24-h physical activity patterns. *Statistical Methods in Medical Research*,
772 096228021986412. <https://doi.org/10.1177/0962280219864125>
- 773 McMeeking, G. R., Kreidenweis, S. M., Baker, S., Carrico, C. M., Chow, J. C., Collett, J. L., et
774 al. (2009). Emissions of trace gases and aerosols during the open combustion of biomass
775 in the laboratory. *Journal of Geophysical Research*, 114(D19).
776 <https://doi.org/10.1029/2009JD011836>
- 777 Ottmar, R. D., Miranda, A. I., & Sandberg, D. V. (2008). Characterizing Sources of Emissions
778 from Wildland Fires. In *Developments in Environmental Science* (Vol. 8, pp. 61–78).
779 Elsevier. Retrieved from <http://www.treesearch.fs.fed.us/pubs/34248>
- 780 Palarea-Albaladejo, J., & Martín-Fernández, J. A. (2015). zCompositions — R package for
781 multivariate imputation of left-censored data under a compositional approach.
782 *Chemometrics and Intelligent Laboratory Systems*, 143, 85–96.
783 <https://doi.org/10.1016/j.chemolab.2015.02.019>
- 784 Palarea-Albaladejo, J., Martín-Fernández, J. A., & Olea, R. A. (2014). A bootstrap estimation
785 scheme for chemical compositional data with nondetects. *Journal of Chemometrics*,
786 28(7), 585–599. <https://doi.org/10.1002/cem.2621>

- 787 Paul, K. T., Hull, T. R., Lebek, K., & Stec, A. A. (2008). Fire smoke toxicity: The effect of
788 nitrogen oxides. *Fire Safety Journal*, *43*(4), 243–251.
789 <https://doi.org/10.1016/j.firesaf.2007.10.003>
- 790 Pawlowsky-Glahn, V., & Buccianti, A. (Eds.). (2011). *Compositional data analysis: theory and*
791 *applications*. Chichester, West Sussex, U.K.: Wiley.
- 792 Pawlowsky-Glahn, V., & Egozcue, J. J. (2001). Geometric approach to statistical analysis on the
793 simplex. *Stochastic Environmental Research and Risk Assessment*, *15*(5), 384–398.
794 <https://doi.org/10.1007/s004770100077>
- 795 Pawlowsky-Glahn, V., Egozcue, J. J., Olea, R. A., & Pardo-Igúzquiza, E. (2015a). Cokriging of
796 compositional balances including a dimension reduction and retrieval of original units.
797 *Journal of the Southern African Institute of Mining and Metallurgy*, *115*, 59–72.
- 798 Pawlowsky-Glahn, V., Egozcue, J. J., & Tolosana-Delgado, R. (2015b). *Modelling and analysis*
799 *of compositional data*. Chichester, West Sussex, U.K.: Wiley.
- 800 Pearson, K. (1896). Mathematical contributions to the theory of evolution.--on a form of
801 spurious correlation which may arise when indices are used in the measurement of
802 organs. *Proceedings of the Royal Society of London (1854-1905)*, *60*(1), 489–498.
803 <https://doi.org/10.1098/rspl.1896.0076>
- 804 Quinn, T. P., Erb, I., Richardson, M. F., & Crowley, T. M. (2018). Understanding sequencing
805 data as compositions: an outlook and review. *Bioinformatics*, *34*(16), 2870–2878.
806 <https://doi.org/10.1093/bioinformatics/bty175>
- 807 R Core Team. (2018). R: A language and environment for statistical computing (Version 3.5.0).
808 Vienna, Austria: R Foundation for Statistical Computing.

- 809 Radke, L., Hegg, D., Lyons, J., Brock, C., Hobbs, P., Weiss, R., & Rasmussen, R. (1988).
810 Airborne measurements on smokes from biomass burning. In P. V. Hobbs & M. P.
811 McCormick (Eds.), *Aerosols and Climate* (pp. 411–422).
- 812 Roberts, J. M., Veres, P., Warneke, C., Neuman, J. A., Washenfelder, R. A., Brown, S. S., et al.
813 (2010). Measurement of HONO, HNCO, and other inorganic acids by negative-ion
814 proton-transfer chemical-ionization mass spectrometry (NI-PT-CIMS): application to
815 biomass burning emissions. *Atmospheric Measurement Techniques*, 3(4), 981–990.
816 <https://doi.org/10.5194/amt-3-981-2010>
- 817 Rockwell, B. G., Girty, G. H., & Rockwell, T. K. (2014). A statistical framework for calculating
818 and assessing compositional linear trends within fault zones: a case study of the NE block
819 of the Clark Segment, San Jacinto Fault, California, USA. *Pure and Applied Geophysics*,
820 171(11), 2919–2935. <https://doi.org/10.1007/s00024-014-0851-6>
- 821 Rogers, J. M., Susott, R. A., & Kelsey, R. G. (1986). Chemical composition of forest fuels
822 affecting their thermal behavior. *Can. J. For. Res.*, 16(4), 721–726.
823 <https://doi.org/10.1139/x86-129>
- 824 Sekimoto, K., Koss, A. R., Gilman, J. B., Selimovic, V., Coggon, M. M., Zarzana, K. J., et al.
825 (2018). High- and low-temperature pyrolysis profiles describe volatile organic compound
826 emissions from western US wildfire fuels. *Atmospheric Chemistry and Physics*, 18(13),
827 9263–9281. <https://doi.org/10.5194/acp-18-9263-2018>
- 828 Shafizadeh, F. (1984). The Chemistry of Pyrolysis and Combustion. In R. Rowell (Ed.), *The*
829 *Chemistry of Solid Wood* (Vol. 207, pp. 489–529). Washington, D.C.: American
830 Chemical Society.

- 831 Shen, G., Xue, M., Wei, S., Chen, Y., Zhao, Q., Li, B., et al. (2013). Influence of fuel moisture,
832 charge size, feeding rate and air ventilation conditions on the emissions of PM, OC, EC,
833 parent PAHs, and their derivatives from residential wood combustion. *Journal of*
834 *Environmental Sciences*, 25(9), 1808–1816. [https://doi.org/10.1016-](https://doi.org/10.1016/S1001-0742(12)60258-7)
835 [0742\(12\)60258-7](https://doi.org/10.1016/S1001-0742(12)60258-7)
- 836 Speranza, A., Caggiano, R., Pavese, G., & Summa, V. (2018). The study of characteristic
837 environmental sites affected by diverse sources of mineral matter using compositional
838 data analysis. *Condensed Matter*, 3(2), 16. <https://doi.org/10.3390/condmat3020016>
- 839 Surawski, N. C., Sullivan, A. L., Roxburgh, S. H., Meyer, C. P. M., & Polglase, P. J. (2016).
840 Incorrect interpretation of carbon mass balance biases global vegetation fire emission
841 estimates. *Nature Communications*, 7, 11536. <https://doi.org/10.1038/ncomms11536>
- 842 Tangren, C. D., McMahon, C. K., & Ryan, P. W. (1976). Chapter II - Contents and effects of
843 forest fire smoke. In *Southern forestry smoke management guidebook* (pp. 9–22).
844 Asheville, NC: USDA Forest Service, Southeastern Forest Experiment Station. Retrieved
845 from <http://www.treesearch.fs.fed.us/pubs/683>
- 846 Templ, M., Hron, K., & Filzmoser, P. (2011). robCompositions: An R-package for robust
847 statistical analysis of compositional data. In V. Pawlowsky-Glahn & A. Buccianti (Eds.),
848 *Compositional Data Analysis* (pp. 341–355). Chichester, UK: John Wiley & Sons, Ltd.
849 <https://doi.org/10.1002/9781119976462.ch25>
- 850 Thió-Henestrosa, S., & Comas, M. (2016, April 20). CoDaPack v2 User's Guide. University of
851 Girona, Dept. of Computer Science and Applied Mathematics. Retrieved from
852 <http://ima.udg.edu/codapack/assets/codapack-manual.pdf>

- 853 Urbanski, S. P. (2013). Combustion efficiency and emission factors for wildfire-season fires in
854 mixed conifer forests of the northern Rocky Mountains, US. *Atmospheric Chemistry and*
855 *Physics*, 13(14), 7241–7262. <https://doi.org/10.5194/acp-13-7241-2013>
- 856 Veres, P., Roberts, J. M., Burling, I. R., Warneke, C., de Gouw, J., & Yokelson, R. J. (2010).
857 Measurements of gas-phase inorganic and organic acids from biomass fires by negative-
858 ion proton-transfer chemical-ionization mass spectrometry. *Journal of Geophysical*
859 *Research*, 115(D23), D23302. <https://doi.org/10.1029/2010JD014033>
- 860 Ward, D. E. (2001). Combustion chemistry and smoke. In E. A. Johnson & K. Miyonishi (Eds.),
861 *Forest Fires: Behavior and Ecological Effects* (pp. 55–77). San Diego, CA: Academic
862 Press. Retrieved from <http://www.doi.org/10.1016/B978-012386660-8/50006-3>
- 863 Ward, D. E., & Hao, W. M. (1991). Projections of emissions from burning of biomass for use in
864 studies of global climate and atmospheric chemistry (p. 19). Presented at the Annual
865 Meeting of the Air and Waste Management Association, Vancouver, British Columbia,
866 Canada: Air and Waste Management Association. Retrieved from
867 <http://www.treesearch.fs.fed.us/pubs/43258>
- 868 Ward, D. E., Clements, H. B., & Nelson, R. M., Jr. (1980). Particulate matter emission factor
869 modeling for fire in southeastern fuels. In *Sixth Conference on Fire and Forest*
870 *Meteorology* (pp. 276–284). Seattle, WA: American Meteorological Society.
- 871 Warneke, C., Roberts, J. M., Veres, P., Gilman, J., Kuster, W. C., Burling, I., et al. (2011). VOC
872 identification and inter-comparison from laboratory biomass burning using PTR-MS and
873 PIT-MS. *International Journal of Mass Spectrometry*, 303(1), 6–14.
874 <https://doi.org/10.1016/j.ijms.2010.12.002>

875 Warton, D. I., Wright, I. J., Falster, D. S., & Westoby, M. (2006). Bivariate line-fitting methods
876 for allometry. *Biological Reviews*, *81*(02), 259.

877 <https://doi.org/10.1017/S1464793106007007>

878 Weise, D. R., Johnson, T. J., & Reardon, J. (2015). Particulate and trace gas emissions from
879 prescribed burns in southeastern U.S. fuel types: Summary of a 5-year project. *Fire*

880 *Safety Journal*, *74*, 71–81. <https://doi.org/10.1016/j.firesaf.2015.02.016>

881 Yokelson, R. J., Susott, R., Ward, D. E., Reardon, J., & Griffith, D. W. T. (1997). Emissions

882 from smoldering combustion of biomass measured by open-path Fourier transform

883 infrared spectroscopy. *Journal of Geophysical Research-Atmospheres*, *102*(D15), 18865–

884 18877. <https://doi.org/10.1029/97JD00852>

885 Yokelson, R. J., Burling, I. R., Gilman, J. B., Warneke, C., Stockwell, C. E., de Gouw, J., et al.

886 (2013). Coupling field and laboratory measurements to estimate the emission factors of

887 identified and unidentified trace gases for prescribed fires. *Atmospheric Chemistry and*

888 *Physics*, *13*(1), 89–116. <https://doi.org/10.5194/acp-13-89-2013>

889

Figure 1.

